ENGINEERING TRANSACTIONS • *Engng. Trans.* • **62**, 4, 423–435, 2014
Polish Academy of Sciences • Institute of Fundamental Technological Research (IPPT PAN)
National Engineering School of Metz (ENIM) • Poznan University of Technology

An Investigation of TNT Equivalence of Hemispherical PE4 Charges

Samuel E. RIGBY[1)], Piotr W. SIELICKI[2)]

[1)] *Department of Civil & Structural Engineering*
University of Sheffield
Mappin Street, Sheffield, S1 3JD, UK
e-mail: sam.rigby@shef.ac.uk

[2)] *Poznan University of Technology*
Institute of Structural Engineering
Piotrowo 5, 60-965 Poznań, Poland
e-mail: piotr.sielicki@put.poznan.pl

The TNT equivalence of an explosive is given as the equivalent mass of TNT required to produce a blast wave of equal magnitude to that produced by a unit weight of the explosive in question. Currently, there is a lack of agreement in the literature on the TNT equivalence (TNT_{eq}) of PE4. This paper presents a combined numerical and experimental investigation of TNT_{eq} for hemispherical PE4 charges in far-field blast events. Experimental results are compared to a series of numerical analyses conducted with different masses of TNT explosive and conclusions are drawn in order to provide a more informed value of TNT_{eq}. It is found that a TNT_{eq} of 1.2 best describes the blast waves produced from PE4 detonations, and this factor is found to be invariant of the distance from the explosive when considering far-field events.

Key words: blast loading, experiment, finite element analysis, TNT equivalence.

1. Introduction

The energetic output and the blast load associated with the detonation of a mass of high explosive will differ depending on the chemical composition of the explosive itself. It is therefore convenient to equate the effects of an explosive to a common material, such as trinitrotoluene (TNT). The TNT equivalence of an explosive (TNT_{eq}) is therefore given as the equivalent mass of TNT required to produce a blast wave of equal magnitude to that produced by a unit weight of the explosive in question [1]. Transforming the mass into that of an equivalent

TNT charge in this manner facilitates the use of the scaled distance parameter relationships found in the literature [2, 3].

Values of TNT_{eq} are well documented for common types of explosive [1, 4, 5], however Cooper [6] states that there are *'large errors inherent in the experimental determination of TNT equivalence'*, hence the accuracy and validity of the published values is questionable. Furthermore, previous researchers have proposed TNT equivalences which change with scaled distance [7–10] rather than a constant value. There is the need, therefore, to better quantify TNT equivalence for commercial explosives.

This paper presents a combined numerical and experimental investigation of TNT equivalence for hemispherical PE4 charges in far-field blast events. Experimental results are compared to a series of numerical analyses conducted using ABAQUS Explicit [11] and LS-DYNA [12] with different assumed values of TNT_{eq} for PE4, and conclusions are drawn in order to provide a more informed value of TNT equivalence.

2. Experimental work

2.1. Experimental setup

This paper presents results from a series of experimental trials conducted by the current authors at the University of Sheffield Blast & Impact Laboratory in Buxton, Derbyshire, UK [13, 14]. 250 g Hemispherical PE4 charges[1)] were centrally detonated on a steel anvil sat on a flat, rigid concrete ground slab, at distances of 4, 6, 8 and 10 m from a large, rigid concrete bunker wall, such that diffraction and fluid-structure interaction effects could be ignored. A Kulite HKM 7 bar pressure gauge was placed near ground level and was rigidly embedded flush with the outside face of the bunker wall, maintaining a smooth, regular reflecting surface for the blast wave to propagate over. Figure 1 shows a labelled photograph of the test arena.

With this arrangement, the pressure gauge would be subjected to the normally reflected pressure, which was recorded using a 16-Bit Digital Oscilloscope at a sample rate of 200 kHz, triggered via a voltage drop in a breakwire embedded in the charge periphery to synchronise the recordings with the detonation. The distance from the centre of the charge to the bunker wall was measured for each test using a Hilti laser range meter and was triangulated against two points on the bunker wall to ensure the charge was orthogonal to the pressure gauge. A summary of the experimental test plan is shown in Table 1.

[1)] PE4 is the British equivalent of C4 and is nominally identical, hence the parameters for PE4 can simply be taken as the published values for C4.

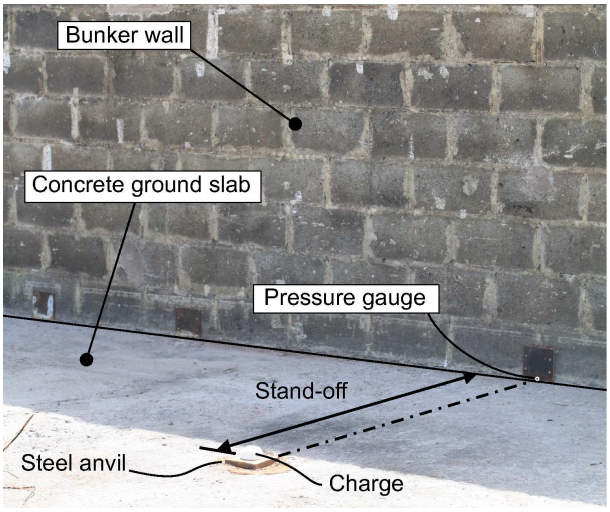

FIG. 1. Labelled photograph of test arena.

Table 1. Summary of experimental tests for hemispherical PE4 explosions.

Test nos.	Explosive	Stand-off [m]	Charge mass [g]
1–3	PE4	4	250
4–6	PE4	6	250
7	PE4	8	250
8	PE4	10	250

2.2. Example result and parameters of interest

Figure 2 shows the experimental trace for test 1 (250 g hemispherical PE4 at 4 m), with relevant blast parameters – peak pressure, positive and negative phase impulse, arrival time and second shock arrival time – labelled. Two features are of note: firstly, there is a small amount of sensor ringing following the arrival of the shock front, making it difficult to discern the true magnitude of peak pressure. Accordingly, the peak pressure is determined from an exponential curve-fit to the recorded data, extrapolated back to the arrival time, details of which can be found in RIGBY *et al.* [14]. Secondly, the second shock can be seen to arrive at the beginning of the negative phase. This is caused by successive reflection of the shock wave off the air/explosives interface shortly after detonation [15], and hence is a useful indicator of the state of the explosive products immediately post-detonation. Indeed, a tertiary shock can be seen to arrive at around 13.5 ms after detonation, however it is small in magnitude and comparable to the overall signal noise and can hence be discounted.

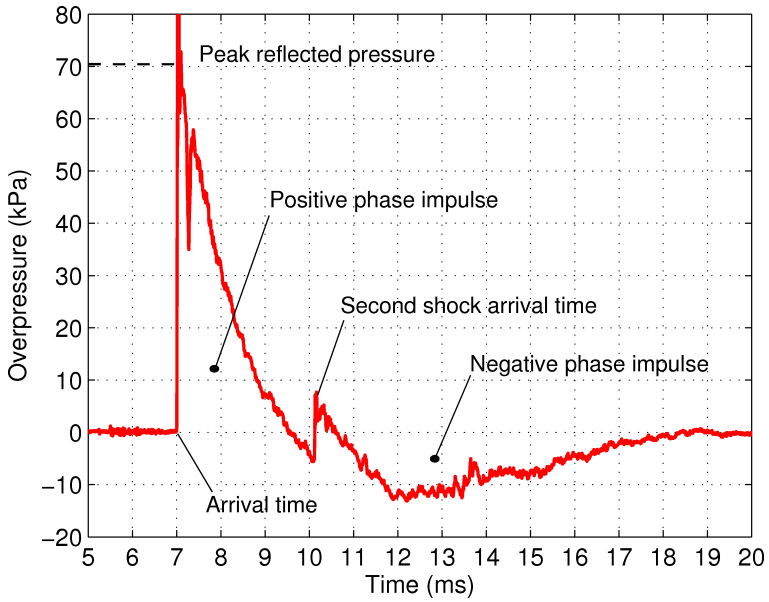

FIG. 2. Example experimental pressure-time history for normally reflected hemispherical 250 g PE4 explosion at 4 m.

3. Numerical analyses

3.1. Model setup

Simulating the rapid pressure evolution associated with the formation a blast wave and the subsequent propagation and interaction with an obstacle is a complex challenge to solve numerically. Analytical solutions for the equations of the motion describing a blast wave [16] are based on a number of underlying assumptions and are not typically of use in design and research. The problem, therefore, requires the use of the finite element method (FEM). In this paper, numerical FEM analyses are performed using ABAQUS Explicit v.6.13 [11] and LS-DYNA v.7.1 [12].

The following governing equations of linear dynamics are solved:

$$
\begin{aligned}
&\text{Equation of motion} && \sigma_{kl,l} + \rho f_k = \rho \ddot{u}_k,\\
&\text{Geometric equation} && \varepsilon_{kl} = 0.5(u_{k,l} + u_{l,k}),\\
&\text{Equation of state} && p = p(\sigma, E_m),\\
&\text{Stress boundary conditions} && \sigma_{kl} n_l = \widehat{t}_k,\\
&\text{Displacement boundary conditions} && u_k = \widehat{u}_k,\\
&\text{Initial conditions} && u_k = \widehat{u}_k^0,\ \dot{u}_k = \widehat{\dot{u}}_k,
\end{aligned}
\tag{3.1}
$$

where $\sigma_{kl,l}$ – stress tensor component; ε_{kl} – strain tensor components; $u_{k,l}$ – derivative component of displacement; n_l – direction; $\widehat{t_k}$ – stress vector; u_k, $\dot{u}_k$ – displacement and velocity components on the edge of the body; ρ – density and E_m – specific energy. In order to link stresses to deformation and internal energy within an element, an equation of state must be specified for each fluid. The ambient air was modelled as an ideal diatomic gas, with $\gamma = 1.4$, see Eq. (3.2):

$$\begin{aligned} p + p_a &= (\gamma - 1)\rho E_m, \\ p + p_a &= \rho R(T - T^z). \end{aligned} \tag{3.2}$$

The term p_a refers to the ambient pressure, ρ is initial air density, R is the universal gas constant, and T^z is the absolute zero on the temperature scale being used. These relations depend on the value of specific internal energy E_m. In order to most accurately reflect reality, the air must be initialised with both of the following: greater than zero internal energy and initial ambient pressure. The value of the ambient pressure is represented by sea level pressure, i.e. ∼101 kPa.

The specific energy, as presented in Eq. (3.3), changes depending on the temperature and can be expressed as the following integral

$$E_m = \int_0^{T-T^z} c_v(T)\, dT + \int_{T_0-T^z}^{T-T^z} c_v(T)\, dT, \tag{3.3}$$

where E_{m0} is the initial specific energy, T_0 is the initial specific energy at room temperature and c_v is the specific heat at constant volume.

The behaviour of condensed charges converting into products of detonation is highly complex and depends strongly on the properties of each explosive. In order to test the method of transforming the charge into an equivalent TNT mass, the explosive and explosion process was explicitly modelled for this study. The widely-used Jones-Wilkins-Lee (JWL) equation of state [17], as presented in Eq. 3.4, was used to describe the expansion of the combustion products.

$$p = A\left(1 - \frac{\omega\rho}{R_1\rho_0}\right)\exp^{\left(-R_1\frac{\rho_0}{\rho}\right)} + B\left(1 - \frac{\omega\rho}{R_2\rho_0}\right)\exp^{\left(-R_2\frac{\rho_0}{\rho}\right)} + \omega\rho E_m. \tag{3.4}$$

The JWL equations describe the pressure generated by chemical energy of the condensed explosive. The constitutive properties: A, B, R_1, R_2, and ω are empirically determined parameters. E_m is the internal specific energy per unit mass and ρ is the instantaneous density of the detonation products. The initial ratio of ρ to ρ_0 used in the JWL equation is assumed to be unity. In this study, the JWL parameters for TNT and PE4 were taken as those given by Dobratz and Crawford [18] and are listed in Table 2.

Table 2. Material model and Equation of State parameters for TNT and PE4, after Dobratz and Crawford [18]. PE4 is equivalent to C4.

Explosive	ρ_0 [kg/m^3]	D [m/s]	PCJ [GPa]	A [GPa]	B [GPa]	R_1 [–]	R_2 [–]	ω [–]	E_m [MJ/kg]
TNT	1630	6930	21.00	371.2	3.231	4.150	0.950	0.300	4.294
PE4	1601	8193	28.00	609.8	12.95	4.500	1.400	0.250	5.621

An image of the numerical model is presented in Fig. 3, which shows the hemispherical explosive charge embedded within an ambient air domain, with rigid ground surface and target labelled. Typically, a high mesh resolution is required to capture the physics associated with the travelling shock – it has been shown that the critical size of the FE mesh should be lower than 50 mm for explosion analysis where the scaled distance is <1.5 m/kg$^{1/3}$ and stand-off is <1 m [19]. In this study, the explosive was meshed with solid elements of 10 mm side length, and the surrounding air was meshed with solid elements of 50 mm side length.

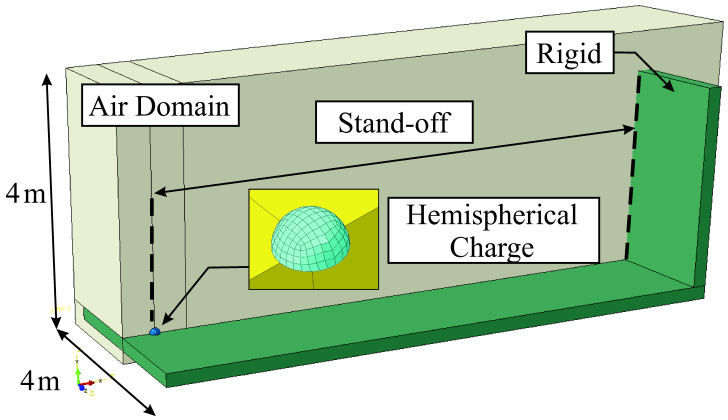

Fig. 3. Numerical domain used in the analyses.

3.2. TNT equivalences tested

In order to test the published values of TNT equivalence for PE4, the following situations were analysed, which have been summarised in Table 3:

- Normal reflection of the blast waves resulting from the detonation of PE4 at 4, 6, 8 and 10 m using the published JWL parameters for C4 (nominally identical to PE4) and 250 g charge mass. This is the control group.
- Assuming an equivalence of 1.19, as suggested by ConWep [1] for impulse equivalence. Charges were therefore modelled as 297.5 g hemispherical

TNT, using the published JWL parameters for TNT. Again normal reflection was analysed for 4, 6, 8 and 10 m stand-off distance.

- Assuming an equivalence of 1.37, as suggested by ConWep for pressure equivalence. Charges were modelled as 342.5 g hemispherical TNT.
- Assuming an averaged value of impulse and pressure equivalence, i.e. $TNT_{eq} = 0.5(1.19 + 1.37) = 1.28$. This is a common approach in the literature, and gives an explosive mass of 320 g TNT.

Table 3. Summary of numerical analyses.

Analysis no.	Explosive	Stand-off [m]	Charge mass [g]	Density [kg/m^3]	Radius [mm]	TNT_{eq}	Condition
1	PE4	4	250	1601	42.09	–	–
2	PE4	6	250	1601	42.09	–	–
3	PE4	8	250	1601	42.09	–	–
4	PE4	10	250	1601	42.09	–	–
5	TNT	4	297.5	1630	44.34	1.19	ConWep impulse equivalence
6	TNT	6	297.5	1630	44.34	1.19	
7	TNT	8	297.5	1630	44.34	1.19	
8	TNT	10	297.5	1630	44.34	1.19	
9	TNT	4	342.5	1630	46.47	1.37	ConWep pressure equivalence
10	TNT	6	342.5	1630	46.47	1.37	
11	TNT	8	342.5	1630	46.47	1.37	
12	TNT	10	342.5	1630	46.47	1.37	
13	TNT	4	320	1630	45.43	1.28	Averaged equivalence
14	TNT	6	320	1630	45.43	1.28	
15	TNT	8	320	1630	45.43	1.28	
16	TNT	10	320	1630	45.43	1.28	

4. Collated results

Figure 4 shows, as an example, the experimental and numerical overpressure-time histories for 250 g PE4 detonated at 8 m stand-off. It is clear from this figure that the choice of TNT_{eq} has a significant influence on both the temporal development and magnitude of blast pressure.

Figures 5–9 show the compiled peak overpressure (i.e. the maximum pressure above ambient conditions), positive phase impulse, negative phase impulse, arrival time and second shock arrival time for experimental and numerical results. The 4 m and 6 m tests were analysed in ABAQUS and the 8 m and 10 m tests were analysed using LS-DYNA. As stated previously, the experimental peak

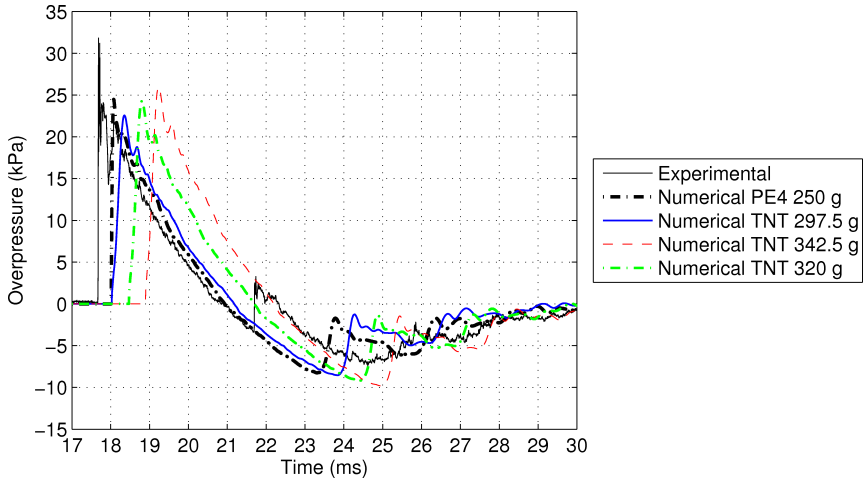

FIG. 4. Experimental and numerical pressure-time histories for normally reflected hemispherical 250 g PE4 explosion at 8 m.

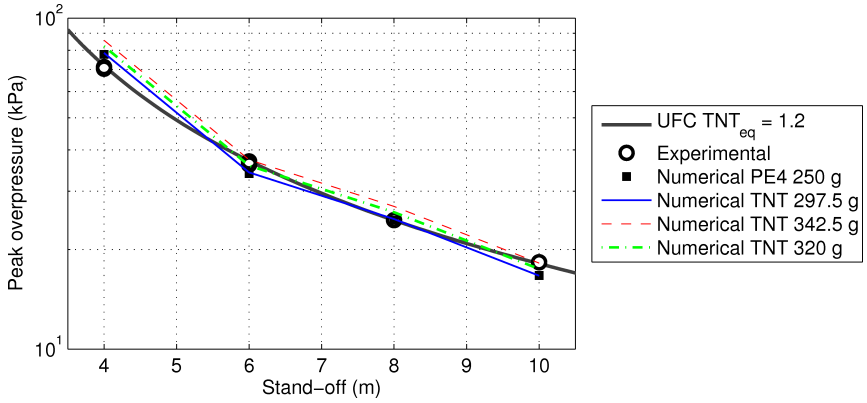

FIG. 5. Compiled numerical and experimental peak overpressure.

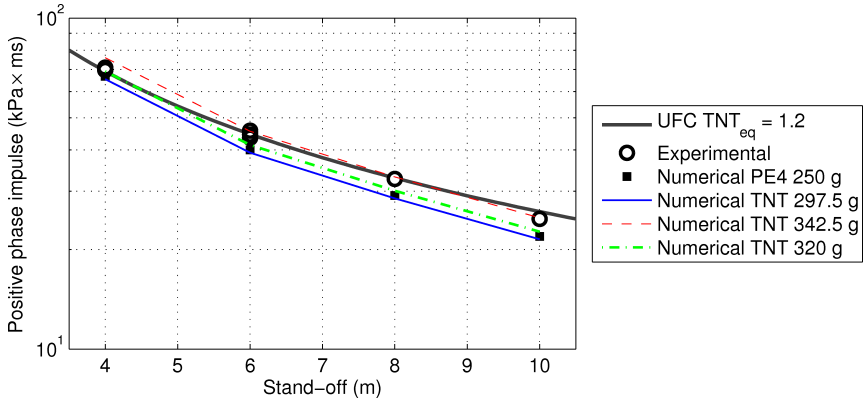

FIG. 6. Compiled numerical and experimental positive phase impulse.

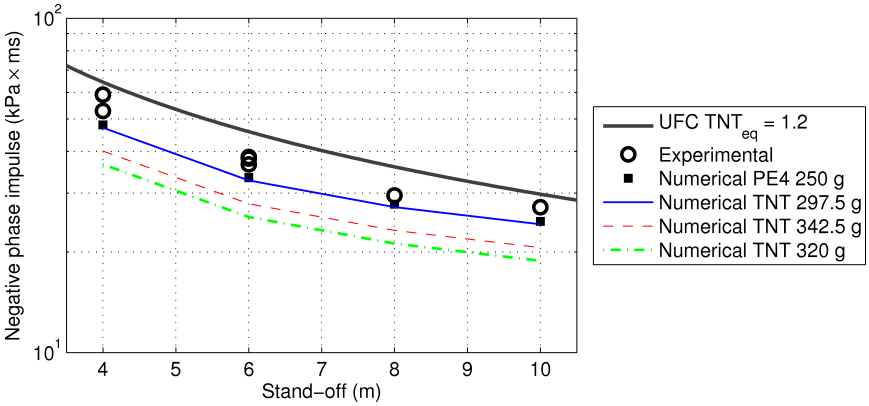

FIG. 7. Compiled numerical and experimental negative phase impulse.

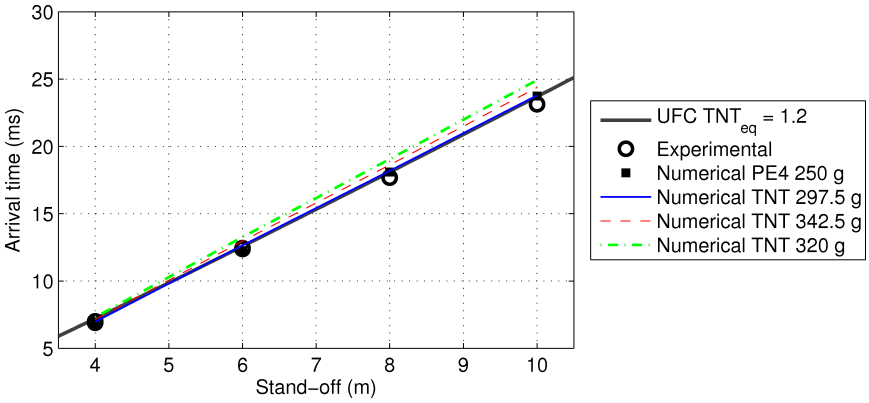

FIG. 8. Compiled numerical and experimental arrival time.

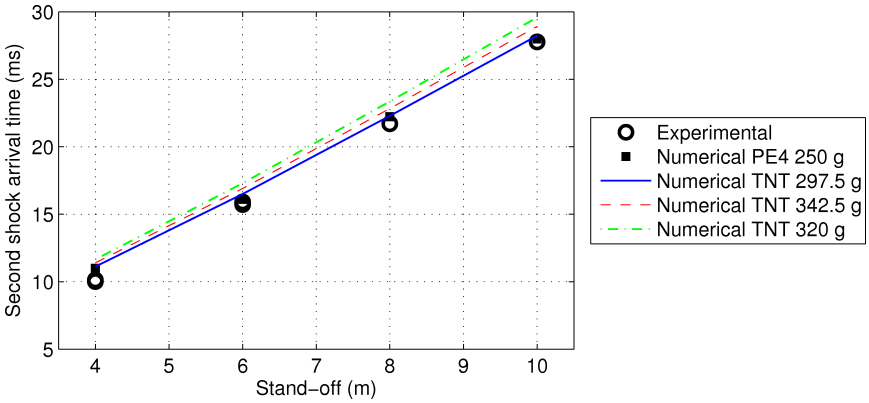

FIG. 9. Compiled numerical and experimental second shock arrival time.

overpressure is determined from fitting an exponential curve to the data and extrapolating back to the arrival time. Primary and secondary shock arrival times are taken directly from the data, and impulses are determined from numerical integration of the recorded data.

Also included in these plots are UFC-3-340-02 [2] semi-empirical parameter predictions assuming a TNT equivalence of 1.2 after Tyas *et al.* [20, 21] and Rigby [22]. Parameter predictions are not available for the second shock as this effect is typically ignored in the literature.

5. Discussion

5.1. One TNT equivalence or two?

The numerical model is able to predict the experimental parameters to a good level of accuracy. In general, the peak pressure is generally over-predicted whilst the impulse is generally under-predicted, albeit still within acceptable engineering tolerance. Whilst this may suggest that two TNT equivalence factors should be used, it is worth being aware of the two following points. Firstly, in almost all cases, the parameters determined from the 297.5 g TNT numerical model offer the best match for the 250 g PE4 analyses. Secondly, the experimental results for 250 g PE4 agree exceptionally well with the semi-empirical UFC-3-340-02 [2] predictions assuming a TNT equivalence of 1.2, with the exception of the negative phase impulse[2)].

This would suggest that the apparent two factor approach for TNT equivalence – if informed by numerical analysis alone – may be misguided. It appears as though any differences in pressure and impulse equivalence may be as a result of slight systemic errors inherent in the numerical model (i.e. numerical dispersion), as opposed to being caused by real life physical effects. This highlights the importance of well-controlled experimental trials when conducting such research.

5.2. Does TNT equivalence change with scaled distance?

According to Cooper [6], if the slope of the pressure wave from a given explosive is different to that of TNT at the same scaled distance, then the peak overpressure from this blast wave will decay at a different rate compared to the TNT wave. This suggests that the value of TNT_{eq} should be expected

[2)] The negative phase is caused by an inertial over-expansion of the air after the passing of the shock wave, and is thus a feature of the air itself rather than the explosive. From the results presented within this paper, as well as those in Ref. [22], it appears as though the properties of the air in expansion are not correctly captured by the numerical model. This is currently being researched by the authors.

to change with increasing distance from the explosive and may explain why previous authors have suggested values which do so. The results presented within this paper demonstrate no such dependence on distance from the explosive.

In the near-field, interaction of the reflected shock front and the interface between the expanding detonation products and the shocked air is known to influence the form of the blast pressure [23]. This interaction is fundamentally dependent on the state of the detonated products in the early stages of expansion (shortly after detonation), and hence we should expect this to change with the explosive type. Once the detonated products have expanded to relative volumes of $\sim$4, however, the JWL equation of state tends towards an ideal gas. Furthermore, once the shock front detaches from the expanding detonation products (which, for the purposes of this study can be assumed to represent far-field conditions), the shock is no longer driven by expansion of the detonation products and hence the only cause for attenuation of the blast wave is through spherical expansion of the shock front through the air. Crucially, this is a geometric property which will scale with the cube-root of the charge mass, i.e. the decay, and hence TNT equivalence, will be geometrically similar regardless of the explosive. This suggests that one value of $\mathrm{TNT_{eq}}$ should be used in the far-field.

The numerical analyses appear to diverge slightly from the experimental results with increasing scaled distance. This implies that as the blast wave propagates through the mesh, more energy is lost. This is perhaps best illustrated in the impulse plot in Fig. 6. The observation is consistent with the fact that we should expect cumulative energy loss through numerical dispersion to occur in our model, which could be improved by increasing the mesh resolution, however one must balance solution accuracy with computational cost. Despite this, the numerical analyses with 297.5 g TNT still offer the best match for the 250 g PE4 analyses and, for the purposes of this study, numerical dispersion effects can be neglected. Also, the UFC-3-340-02 predictions with $\mathrm{TNT_{eq}} = 1.2$ still match the experimental measurements remarkably well at the 10 m stand-off. It has therefore been shown in this paper that a constant TNT equivalence of 1.2 is suitable for PE4 for far-field events.

6. Summary

The TNT equivalence of an explosive is given as the equivalent mass of TNT required to produce a blast wave of equal magnitude to that produced by a unit weight of the explosive in question. Currently, there is a lack of agreement in the literature on the TNT equivalence ($\mathrm{TNT_{eq}}$) of PE4.

A series of experiments were conducted where normally reflected blast parameters (peak overpressure, positive and negative phase impulse and primary shock and second shock arrival time) were measured for 250 g hemispherical

PE4 explosive charges detonated 4, 6, 8 and 10 m from an effectively rigid and semi-infinite bunker wall. Numerical analyses were conducted using ABAQUS Explicit v.6.13 and LS-DYNA v.7.1 for 250 g PE4 and 297.5 g, 320 g and 342.5 g hemispherical TNT charges. These equate to TNT equivalence values of 1.19, 1.28 and 1.37 respectively. From consideration of the collated experimental and numerical results, a TNT equivalence of $\sim$1.2 was found to best represent the experimental and numerical PE4 data.

The results show that this value is suitable for both pressure and impulse equivalence, and that this value is also invariant of distance from the explosive, providing the shock front has detached from the detonation products (i.e. far-field blast events).

Acknowledgment

This work is partially supported by the Polish National Centre for Research and Development under Grant UOD-DEM-1-203/001.

References

1. Hyde D.W., *Conventional Weapons Program (ConWep)*, U.S Army Waterways Experimental Station, Vicksburg, MS, USA, 1991.
2. US Department of Defence, *Structures to resist the effects of accidental explosions*, US DoD, Washington DC, USA, UFC-3-340-02, 2008.
3. Kingery C.N., Bulmash G., *Airblast parameters from TNT spherical air burst and hemispherical surface burst*, Technical Report ARBRL-TR-02555, U.S Army BRL, Aberdeen Proving Ground, MD, USA, 1984.
4. Formby S.A., Wharton R.K., *Blast characteristics and TNT equivalence values for some commercial explosives detonated at ground level*, Journal of Hazardous Materials, **50**, 2–3, 183–198, 1996.
5. Sochet I., Gardebas D., Calderara S., Marchal Y., Longuet B., *Blast wave parameters for spherical explosives detonation in free air*, Open Journal of Safety Science and Technology, **10**, 31–42, 2011.
6. Cooper P.W., *Comments on TNT Equivalence*, [in:] 20th International Pyrotechnics Seminar, pages 1–26, Colorado Springs, CO, USA, 1994.
7. Swisdak M.M., *Explosion effects and properties. Part I – explosion effects in air*, Technical Report NSWC/WOL/TR 75-116, Naval Surface Weapons Center, MD, USA, 1975.
8. Locking P.M., *The trouble with TNT equivalence*, [in:] 26th International Symposium on Ballistics, Miami, FL, USA, 2011.
9. Ackland K., Bornstein H., Lamos D., *An analysis of TNT equivalencies using AUTODYN*, Journal of Explosion Engineering, **1**, 3, 71, 2012.
10. Pachman J., Matyáš R., Künzel M., *Study of TATP: blast characteristics and TNT equivalency of small charges*, Shock Waves, **24**, 4, 439–445, 2014.

11. ABAQUS, v.6.13, *Documentation Collection*, 2012.

12. LS-DYNA, *Theory Manual*, Livermore Software Technology Corporation, CA, USA, 2006.

13. Rigby S.E., Tyas A., Bennett T., Clarke S.D., Fay S.D., *The negative phase of the blast load*, International Journal of Protective Structures, **5**, 1, 1–20, 2014.

14. Rigby S.E., Tyas A., Fay S.D., Clarke S.D., Warren J.A., *Validation of semi-empirical blast pressure predictions for far field explosions – is there inherent variability in blast wave parameters?*, [in:] 6th International Conference on Protection of Structures against Hazards, Tianjin, China, 2014.

15. Baker W.E., *Explosions in air*, University of Texas Press, Austin, TX, USA, 1973.

16. Brode H.L., *Numerical solutions of spherical blast waves*, Journal of Applied Physics, **26**, 6, 766–775, 1955.

17. Lee E.L., Hornig H.C., Kury J.W., *Adiabatic expansion of high explosive detonation products*, Technical Report TID 4500-UCRL 50422, Lawrence Radiation Laboratory, University of California, CA, USA, 1968.

18. Dobratz B.M., Crawford P.C., *LLNL explosives handbook – properties of chemical explosives and explosive simulants*, Technical Report UCRL 52997, Lawrence Livermore National Laboratory, University of California, CA, USA, 1985.

19. Sielicki P.W., *Masonry Failure under Unusual Impulse Loading*, Publishing House of Poznan University of Technology, Poznan, 2013, ISBN 978-83-7775-274-6.

20. Tyas A., Warren J., Bennett T., Fay S., *Prediction of clearing effects in far-field blast loading of finite targets*, Shock Waves, **21**, 2, 111–119, 2011.

21. Tyas A., Bennett T., Warren J.A., Fay S.D., Rigby S.E., *Clearing of blast waves on finite-sized targets – an overlooked approach*, Applied Mechanics and Materials, **82**, 669–674, 2011.

22. Rigby S.E., *Blast Wave Clearing Effects on Finite-Sized Targets Subjected to Explosive Loads*, PhD Thesis, University of Sheffield, UK, 2014.

23. Rigby S.E., Tyas A., Clarke S.D., Fay S.D., Warren J.A., Elgy I., Gant M., *Testing apparatus for the spatial and temporal pressure measurements from near-field free air explosions*, [in:] 6th International Conference on Protection of Structures against Hazards, Tianjin, China, 2014.